10.1071/CH16667_AC

Australian Journal of Chemistry

SUPPLEMENTARY MATERIAL

Rates of water exchange in 2,2'-bipyridine and 1,10-phenanthroline complexes of Co(II) and Mn(II)

Shravan S. Acharya,[a] Bjørn Winther-Jensen,[b] Leone Spiccia[a] and C. André Ohlin[a,c,*]
[a]*School of Chemistry, Monash University, Victoria 3800 Australia*
[b]*Department of Advanced Science and Chemistry, Waseda University, Tokyo, Japan*
[c]*Department of Chemistry, Faculty of Science and Technology, Umeå University, Sweden*
*Email: andre.ohlin@umu.se

Contents

Supporting information

1. Materials and methods

1.1. Sample preparation

All stock solutions were prepared in degassed double-distilled water. $Mn(NO_3)_2{\cdot}4\,H_2O$, $Co(NO_3)_2{\cdot}6\,H_2O$, 1,10-phenanthroline (phen) and 2,2'-bipyridine (bpy) obtained from Sigma-Aldrich were used without further purification. $NaNO_3$ and KCl were employed as background salts. All solutions were freshly prepared before use and purged thoroughly with N_2, and solutions containing cobalt were only handled in N_2 purged septum-sealed NMR tubes, in order to avoid contamination with oxygen, which can lead to the formation of peroxides.[1] The speciations of the solutions were computed with the Hyperquad Simulation and Speciation software (v. 4.0.31) (HySS2009),[2] using stability constants and enthalpies from the literature.[3, 4] See figures 1-2 for example speciation diagrams at 298.15 K.

Solutions with metal to ligand ratios of 1:0, 1:0.5 and 1:2.6, with total metal concentrations of 10 mM in the case of Co(II) and 0.5 mM for Mn(II), were prepared by adding an acidified (HNO_3, pH 1.5) stock solution of either bpy or phen to a stock solution of cobalt or manganese hexa-aqua nitrate (100 mM), and diluting with 0.1 M $NaNO_3$ to reach the desired concentration. The pH was then adjusted to 3.0 by addition of HNO_3. NMR samples were spiked with 5 μl 20% ^{17}O-enriched water (Cambridge Isotopes). NMR samples were allowed to equilibrate at least 16 hours at room temperature before measurements to allow for equilibration.

1.2. Kinetics of $H_2{}^{17}O$ exchange and treatment of data

Nuclear magnetic measurements were carried out on a Bruker Avance DRX 400 (9.7 T, ^{17}O 54.3MHz) spectrometer equipped with a 5 mm broadband probe. Temperature measurements were conducted using a Omega thermocouple reader connected to a dummy sample containing $NaNO_3$ (0.1M) in D_2O with two non-magnetic T-type thermocouples immersed in it at different heights. Spectra were acquired with a pulse width of $\frac{\pi}{2}$, a recycle delay of 500 ms, and were averaged over 256-512 scans. Reference line widths, ν_{ref}, were recorded on a diamagnetic reference sample containing 0.1M $NaNO_3$ and adjusted to pH 3.0 using HNO_3. All samples were equilibrated at the set temperature before the measurements were carried out. Spectra and activation parameters were fitted using gnuplot (v. 4.6.6).[5]

Line widths were fitted using the script in listing 1. An example of the output is given in figure 3.

1.3. Swift and Connick formalism

Swift and Connick showed that when the main source of excess line broadening – $\nu_{\frac{1}{2}} = \nu_{\frac{1}{2},obs} - \nu_{\frac{1}{2},ref}$, where $\nu_{\frac{1}{2},obs}$ is the linewidth of the paramagnetic sample and $nu_{\frac{1}{2},ref}$ is the linewidth of a sample lacking a paramagnetic ion but otherwise identical– of the solvent water signal was related to water exchange on a paramagnetic ion, the relationship could be written as eq. 1, where $\frac{1}{\pi T_{2p}} = \nu_{obs} - \nu_{ref}$, yielding equation 2. Since the effect is additive, we can write eq. 3, where i denotes the species. Using the Eyring-Polanyi expression of the rate as a function of the activation entropy and enthalpy, it is possible to write eq. 4. P_M is defined as the ratio of bound water to a specific species relative to the concentration of free solvent water. k_B, h and R are the Boltzmann constant, Planck's constant and the Universal Gas constant, respectively.

$$\frac{1}{T_{2p}} = P_M \cdot k_m \Leftrightarrow \tag{1}$$

$$\nu_{\frac{1}{2}} = \frac{1}{\pi} P_M \cdot k_m \tag{2}$$

$$\sum_i \Delta\nu^i_{\frac{1}{2}} = \frac{1}{\pi} \sum_i P^i_m k^i_m \tag{3}$$

$$\sum_i \Delta\nu^i_{\frac{1}{2}} = \frac{1}{\pi} \frac{k_b}{h} T \sum_i p^i_m \frac{e^{\frac{\Delta S^i}{R}}}{e^{\frac{\Delta H^i}{R \cdot T}}} \tag{4}$$

$\nu_{\frac{1}{2}}^{obs}$ is also defined as shown in eq. 5

$$\Delta\nu_{\frac{1}{2}}^{obs} = \sum_i \Delta\nu_{\frac{1}{2}}^{i} \tag{5}$$

By measuring the temperature dependent changes in the excess line width, the rates of exchange can be determined as long as P_M is known. It is important to note the importance of the diamagnetic reference sample, which must be otherwise identical to the sample being studied. In other words, reference samples must be maintained at the same pH, ionic strength and temperature as the paramagnetic sample in order to correct for these effects, and to correct for imperfect shimming.

All reported errors in tables are fitting errors (σ).

Multivariate fitting of the excess line widths to determine the thermodynamic parameters was done using equation 4 and gnuplot.[5]

We use only data from the temperature region where there is a linear relationship between excess width and exchange rates. Some previous studies have used the full region, which adds extra degrees of freedom to the point where it is not possible to reliably do global fits for multi-component systems such as those investigated in this study, even using the reduced Swift-Connick relationship (eq. 1). We have previously discussed the general use of this simplified version,[6] and more specifically the issues that need to be considered when applying the full Swift-Connick relationship for a manganese system.[7]

1.4. Temperature effects on speciation

Temperature effects on the speciation was calculated by using the Eyring-Polanyi equation and assuming that the equilibrium entropies and enthalpies were temperature insensitive (see equations 6-8). The equilibrium constant is given by K_T and the stepwise formation constants as β_n, where ΔH and ΔS represent the corresponding enthalpy and entropy of formation.

$$K = \frac{k_B T}{h} e^{-\frac{1}{RT}\left(\Delta H^{\ddagger} - T\Delta S^{\ddagger}\right)} \tag{6}$$

The equilibrium constant at T_2 can be calculated if the equilibrium constant at T_1 and the entropy are known (eq. 7), and from the equilibrium constants the stability constants can be derived (eq. 8).

$$\log_e K_{T_2} = \log_e K_{T_1} + \frac{\Delta H}{R} \cdot \left(\frac{1}{T_1} - \frac{1}{T_2}\right) \tag{7}$$

$$\log_e \beta_n = \sum_{i=1}^{n} \log_e K_i \tag{8}$$

Using the temperature corrected stability constants, temperature dependent P_M can be calculated. See tables 1-7 for the temperature-corrected P_M used in this study. Temperature dependent line widths for different species are shown in figures 4-7.

2. Tables and figures

2.1. Speciation

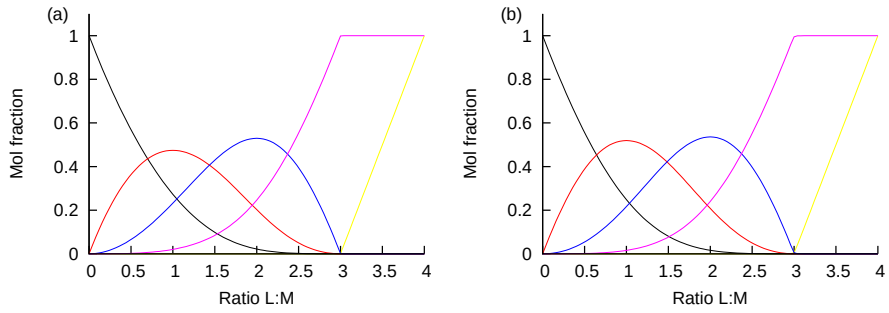

Figure 1: Speciation diagrams for Co:phen (a) and Co:bpy (b) systems at 298.15 K. Mol fractions of L, M, ML, ML_2 and ML_3 given as yellow, black, red, blue, and purple lines, respectively.

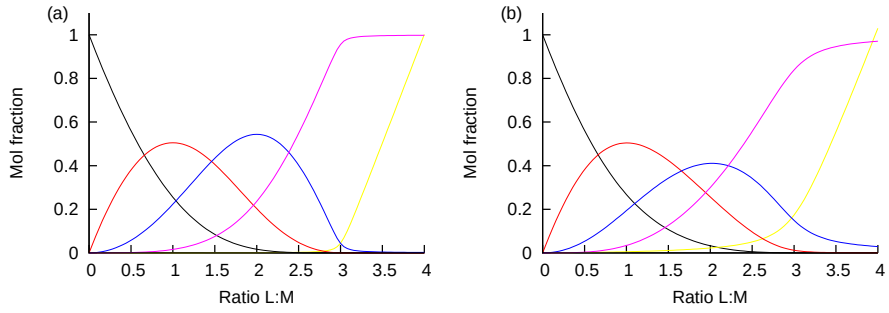

Figure 2: Speciation diagrams for Mn:phen (a) and Mn:bpy (b) systems at 298.15 K. Mol fractions of L, M, ML, ML_2 and ML_3 given as yellow, black, red, blue, and purple lines, respectively.

Table 1: Molar concentrations of $[Co(H_2O)_6]^{2+}$ (M_{free}), $[Co(H_2O)_4(bpy)]^{2+}$ (ML) and $[Co(H_2O)_2(bpy)_2]^{2+}$ (ML_2), and P_{M_0} ($[Co(H_2O)_6]^{2+}$), P_{M_1} ($[Co(H_2O)_4(bpy)]^{2+}$) and P_{M_2} ($[Co(H_2O)_2(bpy)_2]^{2+}$) as functions of temperature. The ratio of Co(II) to bpy is 1:0.5, with a total Co(II) concentration of 10 mM.

T (K)	M_{free} (M)	P_{M_0}	ML (M)	P_{M_1}	ML_2 (M)	P_{M_2}
270.3	5.39×10^{-3}	5.82×10^{-4}	4.22×10^{-3}	3.04×10^{-4}	3.78×10^{-4}	1.36×10^{-5}
272.5	5.41×10^{-3}	5.84×10^{-4}	4.19×10^{-3}	3.02×10^{-4}	3.93×10^{-4}	1.42×10^{-5}
277.6	5.45×10^{-3}	5.88×10^{-4}	4.12×10^{-3}	2.97×10^{-4}	4.29×10^{-4}	1.54×10^{-5}
278.3	5.45×10^{-3}	5.89×10^{-4}	4.11×10^{-3}	2.96×10^{-4}	4.34×10^{-4}	1.56×10^{-5}
281.2	5.47×10^{-3}	5.91×10^{-4}	4.06×10^{-3}	2.92×10^{-4}	4.54×10^{-4}	1.64×10^{-5}
285.5	5.51×10^{-3}	5.95×10^{-4}	4.00×10^{-3}	2.88×10^{-4}	4.85×10^{-4}	1.75×10^{-5}
286.2	5.51×10^{-3}	5.95×10^{-4}	3.99×10^{-3}	2.87×10^{-4}	4.90×10^{-4}	1.76×10^{-5}
289.9	5.54×10^{-3}	5.99×10^{-4}	3.93×10^{-3}	2.82×10^{-4}	5.16×10^{-4}	1.86×10^{-5}
292.8	5.57×10^{-3}	6.01×10^{-4}	3.88×10^{-3}	2.8×10^{-4}	5.36×10^{-4}	1.93×10^{-5}
300.0	5.63×10^{-3}	6.08×10^{-4}	3.77×10^{-3}	2.71×10^{-4}	5.86×10^{-4}	2.11×10^{-5}
304.3	5.66×10^{-3}	6.12×10^{-4}	3.67×10^{-3}	2.64×10^{-4}	6.15×10^{-4}	2.12×10^{-5}
309.4	5.71×10^{-3}	6.16×10^{-4}	3.62×10^{-3}	2.60×10^{-4}	6.47×10^{-4}	2.33×10^{-5}
314.4	5.75×10^{-3}	6.21×10^{-4}	3.54×10^{-3}	2.55×10^{-4}	6.79×10^{-4}	2.44×10^{-5}
324.5	5.84×10^{-3}	6.31×10^{-4}	3.37×10^{-3}	2.43×10^{-4}	7.37×10^{-4}	2.65×10^{-5}

Table 2: Molar concentrations of $[Co(H_2O)_6]^{2+}$ (M_{free}), $[Co(H_2O)_4(bpy)]^{2+}$ (ML) and $[Co(H_2O)_2(bpy)_2]^{2+}$ (ML_2), and P_{M_0} ($[Co(H_2O)_6]^{2+}$), P_{M_1} ($[Co(H_2O)_4(bpy)]^{2+}$) and P_{M_2} ($[Co(H_2O)_2(bpy)_2]^{2+}$) as functions of temperature. The ratio of Co(II) to bpy is 1:2.6, with a total Co(II) concentration of 10 mM.

T (K)	M_{free} (M)	P_{M_0}	ML (M)	P_{M_1}	ML_2 (M)	P_{M_2}
270.3	1.9×10^{-6}	2.05×10^{-7}	2.49×10^{-4}	1.79×10^{-5}	3.74×10^{-3}	1.35×10^{-4}
272.5	2.12×10^{-6}	2.29×10^{-7}	2.54×10^{-4}	1.83×10^{-5}	3.7×10^{-3}	1.33×10^{-4}
277.6	2.75×10^{-6}	2.97×10^{-7}	2.69×10^{-4}	1.93×10^{-5}	3.61×10^{-3}	1.30×10^{-4}
278.3	2.85×10^{-6}	3.08×10^{-7}	2.707×10^{-4}	1.95×10^{-5}	3.60×10^{-3}	1.30×10^{-4}
281.2	3.31×10^{-6}	3.58×10^{-7}	2.80×10^{-4}	2.02×10^{-5}	3.60×10^{-3}	1.30×10^{-4}
285.5	4.15×10^{-6}	4.48×10^{-7}	2.95×10^{-4}	2.12×10^{-5}	3.50×10^{-3}	1.26×10^{-4}
286.2	4.30×10^{-6}	4.65×10^{-7}	2.97×10^{-4}	2.14×10^{-5}	3.49×10^{-3}	1.26×10^{-4}
289.9	5.17×10^{-6}	5.58×10^{-7}	3.10×10^{-4}	2.23×10^{-5}	3.45×10^{-3}	1.24×10^{-4}
292.8	5.97×10^{-6}	6.45×10^{-7}	3.21×10^{-4}	2.31×10^{-5}	3.41×10^{-3}	1.23×10^{-4}
300.0	8.48×10^{-6}	9.15×10^{-7}	3.50×10^{-4}	2.51×10^{-5}	3.33×10^{-3}	1.20×10^{-4}
304.3	1.04×10^{-5}	1.12×10^{-6}	3.66×10^{-4}	2.64×10^{-5}	3.29×10^{-3}	1.18×10^{-4}
309.4	1.30×10^{-5}	1.41×10^{-6}	3.85×10^{-4}	2.77×10^{-5}	3.24×10^{-3}	1.16×10^{-4}
314.4	1.62×10^{-5}	1.75×10^{-6}	4.06×10^{-4}	2.92×10^{-5}	3.18×10^{-3}	1.14×10^{-4}
324.5	2.43×10^{-5}	2.62×10^{-6}	4.44×10^{-4}	3.20×10^{-5}	3.07×10^{-3}	1.11×10^{-4}

Table 3: Molar concentrations of $[Co(H_2O)_6]^{2+}$ (M_{free}), $[Co(H_2O)_4(phen)]^{2+}$ (ML) and $[Co(H_2O)_2(phen)_2]^{2+}$ (ML_2), and P_{M_0} ($[Co(H_2O)_6]^{2+}$), P_{M_1} ($[Co(H_2O)_4(phen)]^{2+}$) and P_{M_2} ($[Co(H_2O)_2(phen)_2]^{2+}$) as functions of temperature. The ratio of Co(II) to phen is 1:0.5, with a total Co(II) concentration of 10 mM.

T (K)	M_{free} (M)	P_{M_0}	ML (M)	P_{M_1}	ML_2 (M)	P_{M_2}
270.3	5.50×10^{-3}	5.94×10^{-4}	4.01×10^{-3}	2.89×10^{-4}	4.84×10^{-4}	1.74×10^{-5}
272.5	5.52×10^{-3}	5.96×10^{-4}	3.98×10^{-3}	2.86×10^{-4}	5.00×10^{-4}	1.80×10^{-5}
278.3	5.57×10^{-3}	6.01×10^{-4}	3.88×10^{-3}	2.79×10^{-4}	5.44×10^{-4}	1.96×10^{-5}
285.5	5.63×10^{-3}	6.08×10^{-4}	3.76×10^{-3}	2.71×10^{-4}	5.97×10^{-4}	2.15×10^{-5}
286.2	5.64×10^{-3}	6.09×10^{-4}	3.75×10^{-3}	2.70×10^{-4}	6.03×10^{-4}	2.17×10^{-5}
289.9	5.67×10^{-3}	6.12×10^{-4}	3.69×10^{-3}	2.65×10^{-4}	6.28×10^{-4}	2.26×10^{-5}
292.8	5.73×10^{-3}	6.19×10^{-4}	3.57×10^{-3}	2.57×10^{-4}	6.81×10^{-4}	2.45×10^{-5}
300.0	5.76×10^{-3}	6.22×10^{-4}	3.51×10^{-3}	2.53×10^{-4}	6.97×10^{-4}	2.51×10^{-5}
304.3	5.80×10^{-3}	6.26×10^{-4}	3.44×10^{-3}	2.48×10^{-4}	7.24×10^{-4}	2.61×10^{-5}
309.4	5.85×10^{-3}	6.32×10^{-4}	3.35×10^{-3}	2.41×10^{-4}	7.54×10^{-4}	2.72×10^{-5}
314.4	5.90×10^{-3}	6.37×10^{-4}	3.27×10^{-3}	2.35×10^{-4}	7.82×10^{-4}	2.81×10^{-5}
324.5	6.00×10^{-3}	6.48×10^{-4}	3.09×10^{-3}	2.23×10^{-4}	8.29×10^{-4}	2.98×10^{-5}

Table 4: Molar concentrations of $[Co(H_2O)_6]^{2+}$ (M_{free}), $[Co(H_2O)_4(phen)]^{2+}$ (ML) and $[Co(H_2O)_2(phen)_2]^{2+}$ (ML_2), and P_{M_0} ($[Co(H_2O)_6]^{2+}$), P_{M_1} ($[Co(H_2O)_4(phen)]^{2+}$) and P_{M_2} ($[Co(H_2O)_2(phen)_2]^{2+}$) as functions of temperature. The ratio of Co(II) to phen is 1:2.6, with a total Co(II) concentration of 10 mM.

T (K)	M_{free} (M)	P_{M_0}	ML (M)	P_{M_1}	ML_2 (M)	P_{M_2}
270.3	1.84×10^{-6}	1.99×10^{-7}	2.01×10^{-4}	1.45×10^{-5}	3.63×10^{-3}	1.31×10^{-4}
272.5	2.16×10^{-6}	2.33×10^{-7}	2.11×10^{-4}	1.52×10^{-5}	3.61×10^{-3}	1.30×10^{-4}
277.6	3.11×10^{-6}	3.36×10^{-7}	2.36×10^{-4}	1.70×10^{-5}	3.55×10^{-3}	1.28×10^{-4}
278.3	3.27×10^{-6}	3.53×10^{-7}	2.40×10^{-4}	1.73×10^{-5}	3.54×10^{-3}	1.28×10^{-4}
281.2	3.98×10^{-6}	4.30×10^{-7}	2.55×10^{-4}	1.83×10^{-5}	3.51×10^{-3}	1.26×10^{-4}
285.5	5.31×10^{-6}	5.73×10^{-7}	2.78×10^{-4}	2.00×10^{-5}	3.46×10^{-3}	1.24×10^{-4}
286.2	5.56×10^{-6}	6.00×10^{-7}	2.82×10^{-4}	2.03×10^{-5}	3.45×10^{-3}	1.24×10^{-4}
289.9	6.98×10^{-6}	7.54×10^{-7}	3.01×10^{-4}	2.17×10^{-5}	3.41×10^{-3}	1.23×10^{-4}
292.8	8.33×10^{-6}	8.99×10^{-7}	3.17×10^{-4}	2.28×10^{-5}	3.37×10^{-3}	1.21×10^{-4}
300.0	1.26×10^{-5}	1.37×10^{-6}	3.57×10^{-4}	2.57×10^{-5}	3.28×10^{-3}	1.18×10^{-4}
304.3	1.60×10^{-5}	1.73×10^{-6}	3.81×10^{-4}	2.74×10^{-5}	3.22×10^{-3}	1.16×10^{-4}
309.4	2.08×10^{-5}	2.24×10^{-6}	4.08×10^{-4}	2.94×10^{-5}	3.15×10^{-3}	1.13×10^{-4}
314.4	2.66×10^{-5}	2.87×10^{-6}	4.35×10^{-4}	3.13×10^{-5}	3.08×10^{-3}	1.11×10^{-4}
324.5	4.17×10^{-5}	4.51×10^{-6}	4.85×10^{-4}	3.49×10^{-5}	2.93×10^{-3}	1.06×10^{-4}

Table 5: Molar concentrations of $[Mn(H_2O)_6]^{2+}$ (M_{free}), $[Mn(H_2O)_4(bpy)]^{2+}$ (ML) and $[Mn(H_2O)_2(bpy)_2]^{2+}$ (ML_2), and P_{M_0} ($[Mn(H_2O)_6]^{2+}$), P_{M_1} ($[Mn(H_2O)_4(bpy)]^{2+}$) and P_{M_2} ($[Mn(H_2O)_2(bpy)_2]^{2+}$) as functions of temperature. The ratio of Mn(II) to bpy is 1:2.6, with a total Mn(II) concentration of 0.5 mM.

T (K)	M_{free} (M)	P_{M_0}	ML (M)	P_{M_1}	ML_2 (M)	P_{M_2}
270.3	4.07×10^{-4}	4.39×10^{-5}	8.93×10^{-5}	6.43×10^{-6}	3.84×10^{-6}	1.38×10^{-7}
272.5	4.03×10^{-4}	4.35×10^{-5}	9.25×10^{-5}	6.66×10^{-6}	4.16×10^{-6}	1.50×10^{-7}
277.6	3.95×10^{-4}	4.27×10^{-5}	1.00×10^{-4}	7.21×10^{-6}	4.03×10^{-6}	1.45×10^{-7}
278.3	3.94×10^{-4}	4.25×10^{-5}	1.01×10^{-4}	7.27×10^{-6}	5.13×10^{-6}	1.85×10^{-7}
281.2	3.89×10^{-4}	4.2×10^{-5}	1.05×10^{-4}	7.58×10^{-6}	5.66×10^{-6}	2.04×10^{-7}
285.5	3.81×10^{-4}	4.12×10^{-5}	1.12×10^{-4}	8.04×10^{-6}	6.54×10^{-6}	2.35×10^{-7}
286.2	3.80×10^{-4}	4.10×10^{-5}	1.13×10^{-4}	8.12×10^{-6}	6.69×10^{-6}	2.41×10^{-7}
289.9	3.74×10^{-4}	4.04×10^{-5}	1.19×10^{-4}	8.51×10^{-6}	7.50×10^{-6}	2.7×10^{-7}
292.8	3.69×10^{-4}	3.98×10^{-5}	1.23×10^{-4}	8.82×10^{-6}	8.19×10^{-6}	2.95×10^{-7}
300.0	3.56×10^{-4}	3.85×10^{-5}	1.33×10^{-4}	9.58×10^{-6}	1.01×10^{-6}	3.64×10^{-7}
304.3	3.49×10^{-4}	3.77×10^{-5}	1.39×10^{-4}	1.00×10^{-5}	1.14×10^{-6}	4.09×10^{-7}
309.4	3.39×10^{-4}	3.67×10^{-5}	1.47×10^{-4}	1.05×10^{-5}	1.30×10^{-6}	4.67×10^{-7}
314.4	3.31×10^{-4}	3.57×10^{-5}	1.53×10^{-4}	1.10×10^{-5}	1.47×10^{-6}	5.29×10^{-7}
324.5	3.14×10^{-4}	3.39×10^{-5}	1.67×10^{-4}	1.20×10^{-5}	1.85×10^{-6}	6.67×10^{-7}

Table 6: Molar concentrations of $[Mn(H_2O)_6]^{2+}$ (M_{free}), $[Mn(H_2O)_4(phen)]^{2+}$ (ML) and $[Mn(H_2O)_2(phen)_2]^{2+}$ (ML_2), and P_{M_0} ($[Mn(H_2O)_6]^{2+}$), P_{M_1} ($[Mn(H_2O)_4(phen)]^{2+}$) and P_{M_2} ($[Mn(H_2O)_2(phen)_2]^{2+}$) as functions of temperature. The ratio of Mn(II) to phen is 1:0.5, with a total Mn(II) concentration of 0.5 mM.

T (K)	M_{free} (M)	P_{M_0}	ML (M)	P_{M_1}	ML_2 (M)	P_{M_2}
270.3	1.15×10^{-3}	1.25×10^{-4}	7.60×10^{-4}	5.47×10^{-5}	8.50×10^{-5}	3.06×10^{-6}
272.5	1.15×10^{-3}	1.25×10^{-4}	7.58×10^{-4}	5.46×10^{-5}	8.69×10^{-5}	3.13×10^{-6}
278.3	1.15×10^{-3}	1.25×10^{-4}	7.52×10^{-4}	5.42×10^{-5}	9.21×10^{-5}	3.31×10^{-6}
285.5	1.16×10^{-3}	1.25×10^{-4}	7.44×10^{-4}	5.36×10^{-5}	9.83×10^{-5}	3.54×10^{-6}
286.2	1.16×10^{-3}	1.25×10^{-4}	7.43×10^{-4}	5.35×10^{-5}	9.89×10^{-5}	3.56×10^{-6}
289.9	1.16×10^{-3}	1.25×10^{-4}	7.39×10^{-4}	5.32×10^{-5}	1.02×10^{-4}	3.67×10^{-6}
292.8	1.16×10^{-3}	1.25×10^{-4}	7.36×10^{-4}	5.30×10^{-5}	1.04×10^{-4}	3.75×10^{-6}
300.0	1.16×10^{-3}	1.25×10^{-4}	7.27×10^{-4}	5.23×10^{-5}	1.10×10^{-4}	3.96×10^{-6}
304.3	1.16×10^{-3}	1.25×10^{-4}	7.22×10^{-4}	5.20×10^{-5}	1.14×10^{-4}	4.09×10^{-6}
309.4	1.16×10^{-3}	1.26×10^{-4}	7.16×10^{-4}	5.15×10^{-5}	1.17×10^{-4}	4.22×10^{-6}
314.4	1.17×10^{-3}	1.26×10^{-4}	7.09×10^{-4}	5.11×10^{-5}	1.21×10^{-4}	4.36×10^{-6}
324.5	1.17×10^{-3}	1.26×10^{-4}	6.97×10^{-4}	5.02×10^{-5}	1.28×10^{-4}	4.61×10^{-6}

Table 7: Molar concentrations of $[Mn(H_2O)_6]^{2+}$ (M_{free}), $[Mn(H_2O)_4(phen)]^{2+}$ (ML) and $[Mn(H_2O)_2(phen)_2]^{2+}$ (ML_2), and P_{M_0} ($[Mn(H_2O)_6]^{2+}$), P_{M_1} ($[Mn(H_2O)_4(phen)]^{2+}$) and P_{M_2} ($[Mn(H_2O)_2(phen)_2]^{2+}$) as functions of temperature. The ratio of Mn(II) to phen is 1:2.6, with a total Mn(II) concentration of 0.5 mM.

T (K)	M_{free} (M)	P_{M_0}	ML (M)	P_{M_1}	ML_2 (M)	P_{M_2}
270.3	3.80×10^{-5}	4.10×10^{-6}	2.19×10^{-4}	1.58×10^{-5}	2.14×10^{-4}	7.70×10^{-6}
272.5	3.67×10^{-5}	3.97×10^{-6}	2.14×10^{-4}	1.54×10^{-5}	2.18×10^{-4}	7.84×10^{-6}
277.6	3.40×10^{-5}	3.67×10^{-6}	2.03×10^{-4}	1.46×10^{-5}	2.26×10^{-4}	8.13×10^{-6}
278.3	3.36×10^{-5}	3.63×10^{-6}	2.02×10^{-4}	1.45×10^{-5}	2.27×10^{-4}	8.17×10^{-6}
281.2	3.22×10^{-5}	3.48×10^{-6}	1.96×10^{-4}	1.41×10^{-5}	2.31×10^{-4}	8.32×10^{-6}
285.5	3.03×10^{-5}	3.27×10^{-6}	1.87×10^{-4}	1.34×10^{-5}	2.37×10^{-4}	8.51×10^{-6}
286.2	2.99×10^{-5}	3.23×10^{-6}	1.85×10^{-4}	1.33×10^{-5}	2.37×10^{-4}	8.55×10^{-6}
289.9	2.85×10^{-5}	3.07×10^{-6}	1.78×10^{-4}	1.28×10^{-5}	2.41×10^{-4}	8.68×10^{-6}
292.8	2.74×10^{-5}	2.95×10^{-6}	1.73×10^{-4}	1.25×10^{-5}	2.44×10^{-4}	8.78×10^{-6}
300.0	2.49×10^{-5}	2.68×10^{-6}	1.60×10^{-4}	1.15×10^{-5}	2.49×10^{-4}	8.97×10^{-6}
304.3	2.35×10^{-5}	2.54×10^{-6}	1.53×10^{-4}	1.10×10^{-5}	2.52×10^{-4}	9.05×10^{-6}
309.4	2.21×10^{-5}	2.39×10^{-6}	1.45×10^{-4}	1.04×10^{-5}	2.53×10^{-4}	9.12×10^{-6}
314.4	2.08×10^{-5}	2.25×10^{-6}	1.38×10^{-4}	9.91×10^{-6}	2.55×10^{-4}	9.16×10^{-6}
324.5	1.87×10^{-5}	2.01×10^{-6}	1.24×10^{-4}	8.94×10^{-6}	2.55×10^{-4}	9.18×10^{-6}

Table 8: Variable temperature ^{17}O NMR line widths for $[Co(H_2O)_6]^{2+}$ (10 mM) in 0.1 M $NaNO_3$ at pH 3.0.

Entry	T (K)	Reference width (Hz)	Width (Hz)[a]	δ (Hz)[a]
1	270.3	98.68±1.45	215.78±0.86	39.9±0.3
2	272.5	92.01±1.35	225.84±0.95	38.7±0.3
3	278.3	75.80±1.04	271.37±1.32	41.2±0.5
4	285.5	70.10±0.91	348.92±1.84	59.5±0.7
5	286.2	64.21±0.84	356.75±2.22	49.4±0.8
6	289.9	56.13±0.68	421.64±2.78	71.7±1.0
7	292.8	52.10±0.61	488.61±3.10	97.7±1.1
8	300.0	44.67±0.49	612.56±4.92	175.3±1.7
9	304.3	40.65±0.46	708.90±6.17	237.8±2.2
10	309.4	36.17±0.38	780.98±7.73	312.8±2.7
11	314.4	32.49±0.33	790.31±8.24	474.4±2.9
12	324.5	27.58±0.27	712.15±6.76	626.2±2.3

[a] Width and signal position of sample; the latter is relative to the reference signal.

2.2. Excess line widths

```
#!/bin/bash
FILE=$1
gnuplot <<- EOF
        set terminal postscript eps enhanced colour
        set output "${FILE}.eps

        set border 3
        set xtics nomirror
        set ytics nomirror

        pi=3.141592653589793

        set samples 5000
        set fit errorvariables

        lor(x)=height*((1/pi)*(0.5*width)/((x-center)**2+(0.5*width)**2))


        set xlabel 'Shift (Hz)'
        set xrange [2000:-2000]
        set ylabel 'Intensity'

        center=100
        width=100
        height=2E6

        fit lor(x) "${FILE}" u 1:2 via width,center,height

        fitinfo = sprintf("fit width, center: %.2f+/-%.2f, %.1f+/-%.1f", width, width_err,
            center,center_err)

        plot "${FILE}" u 1:2 w lines lt -1 ti 'obs',\
               lor(x) w lines lt 1 t fitinfo,\
               '' u 1:(lor(\$1)-\$2) w lines lt 3 ti 'residual'

EOF
```

Listing 1: Lorentzian fitting script written in bash and octave.

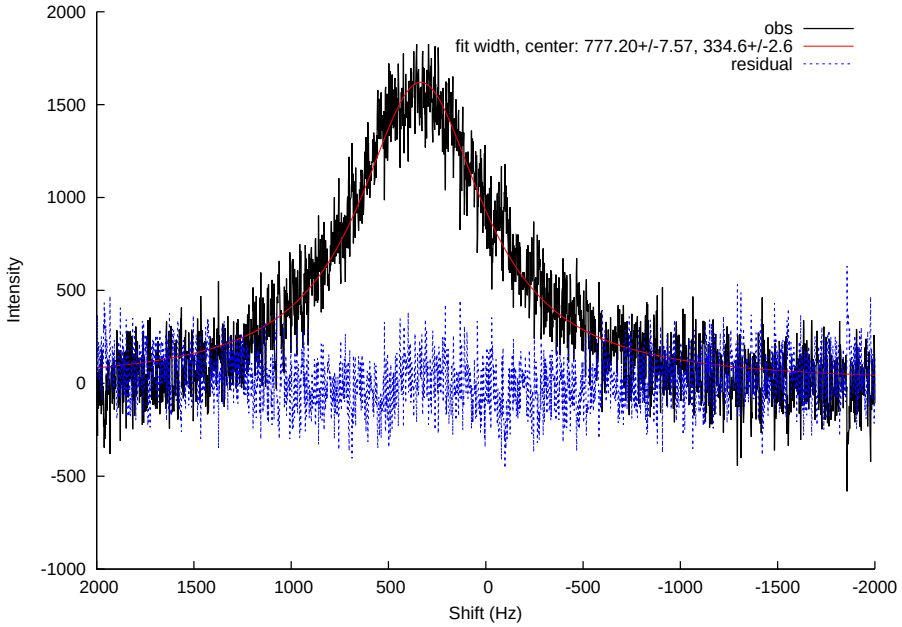

Figure 3: Example of fitted spectrum using the code in listing 1.

Table 9: Variable temperature ^{17}O NMR line widths for Co(II):phen in a 1:0.5 ratio ([Co(II)]=10 mM) in 0.1 M $NaNO_3$ at pH 3.0.

Entry	T (K)	Reference width (Hz)	Width (Hz)[a]	δ (Hz)[a]
1	270.3	98.68±1.45	204.22±0.88	38.4±0.3
2	272.5	92.01±1.35	209.04±0.97	38.8±0.3
3	278.3	75.80±1.04	251.18±1.40	39.0±0.5
4	285.5	70.10±0.91	316.33±1.68	61.2±0.6
5	286.2	64.21±0.84	334.50±1.80	59.6±0.6
6	289.9	56.13±0.68	388.13±2.58	71.0±0.9
7	292.8	52.10±0.61	447.60±3.15	83.0±1.1
8	300.0	44.67±0.49	605.17±8.28	182.1±2.9
9	304.3	40.65±0.46	689.88±10.27	220.7±3.6
10	309.4	36.17±0.38	742.29±11.61	338.9±4.1
11	314.4	32.49±0.33	707.45±12.07	457.0 ±4.2
12	324.5	27.58±0.27	660.11±9.92	642.6±3.5

[a] Width and signal position of sample; the latter is relative to the reference signal.

Table 10: Variable temperature ^{17}O NMR line widths for Co(II):phen in a 1:2.6 ratio ([Co(II)]=10 mM) in 0.1 M $NaNO_3$ at pH 3.0.

Entry	T (K)	Reference width (Hz)	Width (Hz)[a]	δ (Hz)[a]
1	270.3	106.89±1.69	115.37±0.32	16.8±0.1
2	272.5	93.47±1.42	111.36±0.29	21.4±0.1
3	277.6	86.71±1.16	105.63±0.23	19.7±0.1
4	278.3	77.41±1.10	103.46±0.28	26.3±0.1
5	281.2	74.25±0.95	101.53±0.24	21.8±0.1
6	285.5	67.83±0.86	102.46±0.24	22.0±0.1
7	286.2	63.56±0.78	103.21±0.25	26.5±0.1
8	289.9	56.48±0.67	106.96±0.28	28.1±0.1
9	292.8	53.64±0.65	113.07±0.37	25.2±0.1
10	300.0	45.03±0.51	129.50±0.46	33.5±0.2
11	304.3	40.09±0.45	144.90±0.49	46.5±0.2
12	309.4	36.98±0.39	161.07±0.62	55.0±0.2
13	314.4	32.71±0.35	166.75±0.76	66.7±0.3
14	324.5	27.19±0.27	155.37±0.66	105.2±0.2

[a] Width and signal position of sample; the latter is relative to the reference signal.

Table 11: Variable temperature ^{17}O NMR line widths for Co(II):bpy in a 1:0.5 ratio ([Co(II)]=10 mM) in 0.1 M $NaNO_3$ at pH 3.0.

Entry	T (K)	Reference width (Hz)	Width (Hz)[a]	δ (Hz)[a]
1	270.3	106.89±1.69	211.87±0.80	32.0±0.3
2	272.5	93.47±1.42	216.68±0.90	34.6±0.3
3	277.6	86.71±1.16	247.73±1.05	42.3±0.4
4	278.3	77.41±1.10	256.37±1.12	53.6±0.4
5	281.2	74.25±0.95	288.79±1.42	47.2±0.5
6	285.5	67.83±0.86	339.77±1.92	56.6±0.7
7	286.2	63.56±0.78	354.94±2.05	62.6±0.7
8	289.9	56.48±0.67	420.22±2.67	94.3±0.9
9	292.8	53.64±0.65	472.70±3.21	121.2±1.1
10	300.0	45.03±0.51	591.11±4.91	200.4±1.7
11	304.3	40.09±0.45	647.74±5.72	293.2±2.0
12	309.4	36.98±0.39	687.62±6.05	378.4±2.1
13	314.4	32.71±0.35	650.94±6.36	488.6±2.2
14	324.5	27.19±0.27	497.90±4.34	624.8±1.5

[a] Width and signal position of sample; the latter is relative to the reference signal.

Table 12: Variable temperature ^{17}O NMR line widths for Co(II):bpy in a 1:2.6 ratio ([Co(II)]=10 mM) in 0.1 M $NaNO_3$ at pH 3.0.

Entry	T (K)	Reference width (Hz)	Width (Hz)[a]	δ (Hz)[a]
1	270.3	106.89±1.69	119.02±0.31	16.4±0.1
2	272.5	93.47±1.42	119.21±0.31	53.6±0.4
3	277.6	86.71±1.16	111.35±0.29	19.5±0.1
4	278.3	77.41±1.10	109.98±0.27	27.0±0.1
5	281.2	74.25±0.95	109.23±0.32	16.9±0.1
6	285.5	67.83±0.86	114.45±0.30	19.5±0.1
7	286.2	63.56±0.78	114.81±0.31	27.1±0.1
8	289.9	56.48±0.67	122.10±0.34	30.2±0.1
9	292.8	53.64±0.65	129.33±0.37	33.3±0.1
10	300.0	45.03±0.51	150.73±0.54	45.3±0.2
11	304.3	40.09±0.45	157.78±0.59	66.1±0.2
12	309.4	36.98±0.39	162.93±0.59	80.9±0.2
13	314.4	32.71±0.35	152.98±0.54	92.6±0.2
14	324.5	27.19±0.27	115.70±0.38	114.1±0.1

[a] Width and signal position of sample; the latter is relative to the reference signal.

Table 13: Variable temperature ^{17}O NMR line widths for $[Mn(H_2O)_6]^{2+}$ (2 mM) in 0.1 M $NaNO_3$ at pH 3.0.

Entry	T (K)	Reference width (Hz)	Width (Hz)[a]	δ (Hz)[a]
1	270.3	98.68±1.45	460.38±2.85	13.0±1.0
2	272.5	92.01±1.35	485.29±3.43	-10.3±1.3
3	278.3	75.80±1.04	611.12±4.74	-3.8±1.7
4	285.5	70.10±0.91	801.56±7.46	0±2.6
5	286.2	64.21±0.84	797.45±7.73	5.4±2.7
6	289.9	56.13±0.68	903.16±7.34	-10.2±2.5
7	292.8	52.10±0.61	1034.56±12.49	5.8±4.3
8	300.0	44.67±0.49	1230.13±18.85	7.6±6.4
9	304.3	40.65±0.46	1451.25±20.42	-31.7±6.8
10	309.4	36.17±0.38	1554.33±23.24	-86.7±7.6
11	314.4	32.49±0.33	1642.91±25.41	19.7±8.1
12	324.5	27.58±0.27	1639.93±24.86	-61.6±8.0

[a] Width and signal position of sample; the latter is relative to the reference signal.

Table 14: Variable temperature ^{17}O NMR line widths for Mn(II):phen in a 1:0.5 ratio ([Mn(II)]=2 mM) in 0.1 M $NaNO_3$ at pH 3.0.

Entry	T (K)	Reference width (Hz)	Width (Hz)[a]	δ (Hz)[a]
1	270.3	98.68±1.45	470.55±2.89	8.9±1.0
2	272.5	92.01±1.35	489.91±3.42	-3.8±1.2
3	278.3	75.80±1.04	621.35±5.18	-16.0±1.8
4	285.5	70.10±0.91	776.81±6.54	12.6±2.3
5	286.2	64.21±0.84	810.11±7.74	-19.0±2.7
6	289.9	56.13±0.68	931.62±10.10	-17.4±3.5
7	292.8	52.10±0.61	1060.73±12.32	-5.3±4.2
8	300.0	44.67±0.49	1289.40±18.88	32.0±6.4
9	304.3	40.65±0.46	1397.11±18.88	25.0±6.3
10	309.4	36.17±0.38	1516.06±23.76	34.8±7.8
11	314.4	32.49±0.33	1551.23±26.53	28.1±8.7
12	324.5	27.58±0.27	1756.73±25.57	21.6±8.1

[a] Width and signal position of sample; the latter is relative to the reference signal.

Table 15: Variable temperature ^{17}O NMR line widths for Mn(II):phen in a 1:2.6 ratio ([Mn(II)]=0.5 mM) in 0.1 M $NaNO_3$ at pH 3.0.

Entry	T (K)	Reference width (Hz)	Width (Hz)[a]	δ (Hz)[a]
1	270.3	106.89±1.69	197.60±0.80	-5.1±0.3
2	272.5	93.47±1.42	199.60±0.82	8.0±0.3
3	277.6	86.71±1.16	214.54±0.79	0.3±0.3
4	278.3	77.41±1.10	219.58±0.86	10.7±0.3
5	281.2	74.25±0.95	235.94±1.07	-2.5±0.4
6	285.5	67.83±0.86	259.48±1.23	-1.0±0.4
7	286.2	63.56±0.78	262.99±1.28	10.6±0.5
8	289.9	56.48±0.67	292.49±1.51	10.5±0.5
9	292.8	53.64±0.65	315.12±1.84	-7.8±0.6
10	300.0	45.03±0.51	409.43±2.22	9.0±0.8
11	304.3	40.09±0.45	408.53±2.68	16.2±0.9
12	309.4	36.98±0.39	448.08±3.14	2.6±1.1
13	314.4	32.71±0.35	469.34±3.56	0.8±1.3
14	324.5	27.19±0.27	456.83±3.68	9.8±1.3

[a] Width and signal position of sample; the latter is relative to the reference signal.

Table 16: Variable temperature ^{17}O NMR line widths for Mn(II):bpy in a 1:0.5 ratio ([Mn(II)]=0.5 mM) in 0.1 M $NaNO_3$ at pH 3.0.

Entry	T (K)	Reference width (Hz)	Width (Hz)[a]	δ (Hz)[a]
1	270.3	106.89±1.69	193.47±0.83	-6.5±0.3
2	272.5	93.47±1.42	197.09±0.81	1.0±0.3
3	277.6	86.71±1.16	212.70±0.81	5.0±0.3
4	278.3	77.41±1.10	218.93±0.87	7.0±0.3
5	281.2	74.25±0.95	230.23±1.01	-1.5±0.4
6	285.5	67.83±0.86	255.80±1.22	1.3±0.4
7	286.2	63.56±0.78	262.94±1.31	2.7±0.5
8	289.9	56.48±0.67	294.08±1.50	10.5±0.5
9	292.8	53.64±0.65	317.48±2.02	-9.4±0.7
10	300.0	45.03±0.51	379.55±2.62	-9.1±0.9
11	304.3	40.09±0.45	416.90±2.84	24.7±1.0
12	309.4	36.98±0.39	460.23±3.28	4.9±1.2
13	314.4	32.71±0.35	471.99±3.63	6.7±1.3
14	324.5	27.19±0.27	464.53±3.81	22.7±1.3

[a] Width and signal position of sample; the latter is relative to the reference signal.

Table 17: Variable temperature ^{17}O NMR line widths for Mn(II):bpy in a 1:2.6 ratio ([Mn(II)]=0.5 mM) in 0.1 M $NaNO_3$ at pH 3.0.

Entry	T (K)	Reference width (Hz)	Width (Hz)[a]	δ (Hz)[a]
1	270.3	106.89±1.69	195.81±0.74	-0.9±0.3
2	272.5	93.47±1.42	199.06±0.82	8.0±0.3
3	277.6	86.71±1.16	215.20±0.84	-0.3±0.3
4	278.3	77.41±1.10	220.55±0.96	4.1±0.3
5	281.2	74.25±0.95	232.73±1.05	-3.1±0.4
6	285.5	67.83±0.86	258.60±1.25	-4.5±0.4
7	286.2	63.56±0.78	267.68±1.29	4.6±0.5
8	289.9	56.48±0.67	298.32±1.58	7.4±0.6
9	292.8	53.64±0.65	325.91±1.96	-4.9±0.7
10	300.0	45.03±0.51	380.50±2.54	3.3±0.9
11	304.3	40.09±0.45	417.13±2.91	17.1±1.0
12	309.4	36.28±0.39	457.32±3.28	3.4±1.2
13	314.4	32.71±0.35	482.20±3.69	2.5±1.3
14	324.5	27.19±0.27	471.23±3.83	5.7±1.3

[a] Width and signal position of sample; the latter is relative to the reference signal.

2.3. Line-width plots

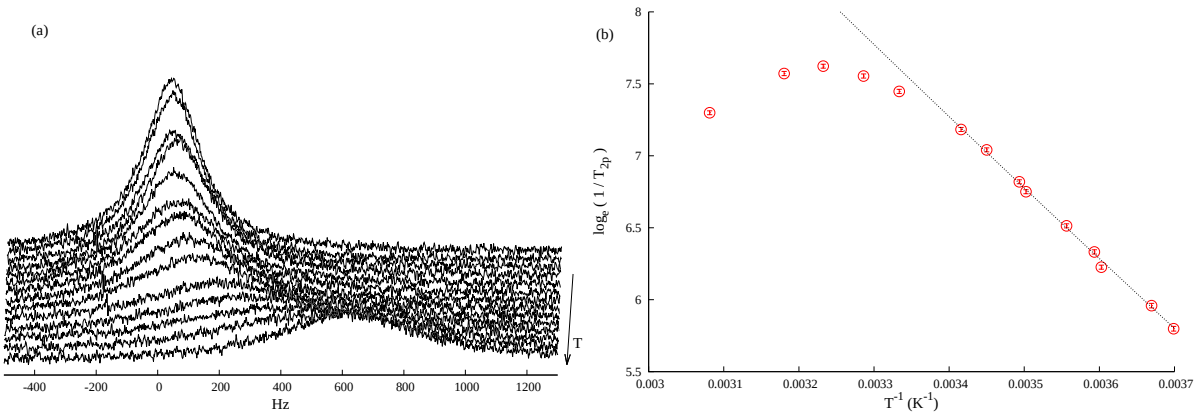

Figure 4: (a) Change in line width and position of free solvent water ^{17}O NMR signal between 270.4 K and 324.6 K (Co(II):bpy 1:0.5; 0.1 M $NaNO_3$; pH 3.0). (b) $\log_e(\frac{1}{T_{2p}})$ *vs* T^{-1} for the signal in (a). The dotted line was constructed using the predicted line width based on the determined activation enthalpies and entropies.

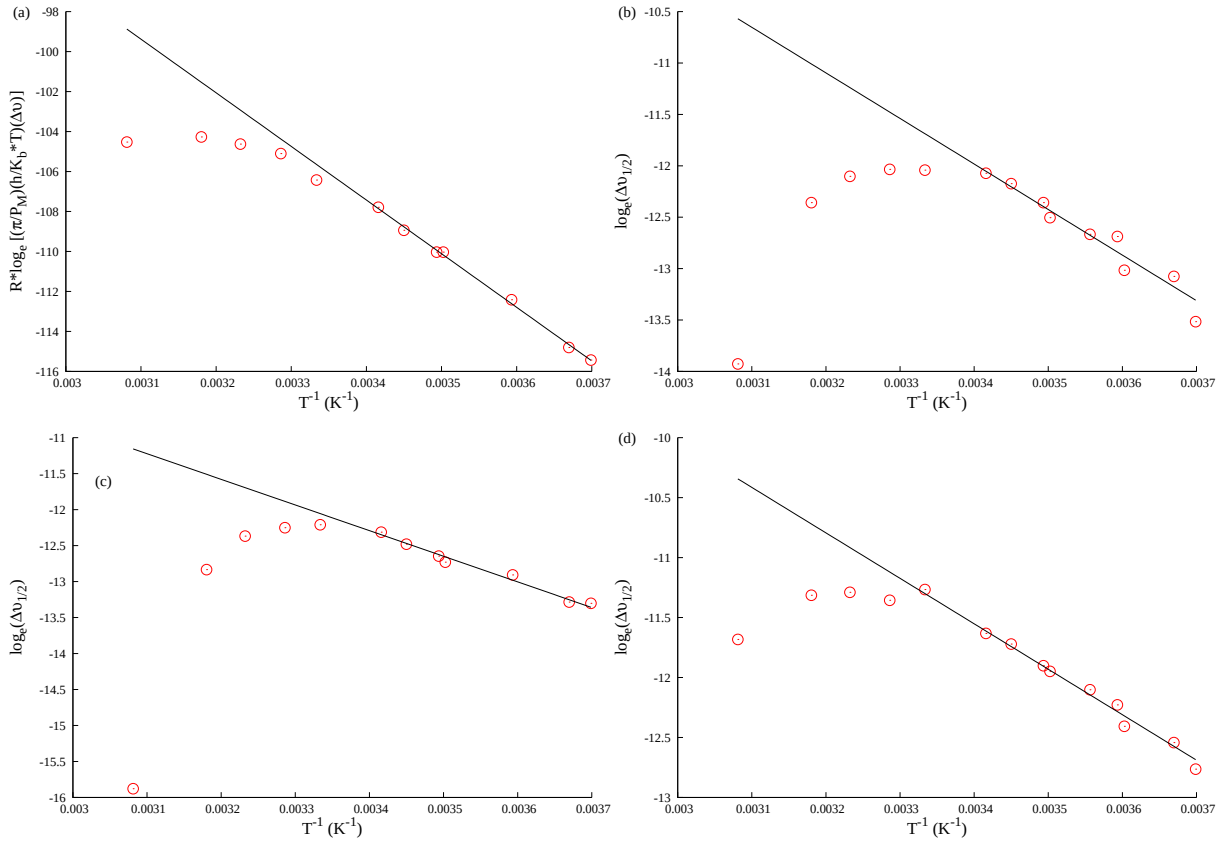

Figure 5: Variable temperature plots for Mn^{2+} solutions showing the contribution of specific species to the line width in different samples. (a) $[Mn(H_2O)_6]^{2+}$ (2 mM) without any added ligand. (b) Mn(II):bpy 1:2.6 ([Mn]=0.5 mM); the contribution of $[Mn(H_2O)_6]^{2+}$ to the excess line width has been subtracted over the entire temperature range so that the contribution of $[Mn(H_2O)_4(bpy)]^{2+}$ is apparent. (c) Mn(II):phen 1:0.5 ([Mn]=2 mM); the contribution of $[Mn(H_2O)_6]^{2+}$ to the excess line width has been subtracted over the entire temperature range so that the contribution of $[Mn(H_2O)_4(phen)]^{2+}$ is apparent (d) Mn(II):phen 1:2.6 ([Mn]=0.5 mM); the contributions of $[Mn(H_2O)_6]^{2+}$ and $[Mn(H_2O)_4(phen)]^{2+}$ to the excess line width has been subtracted over the entire temperature range so that the contribution of $[Mn(H_2O)_2(phen)_2]^{2+}$ is apparent

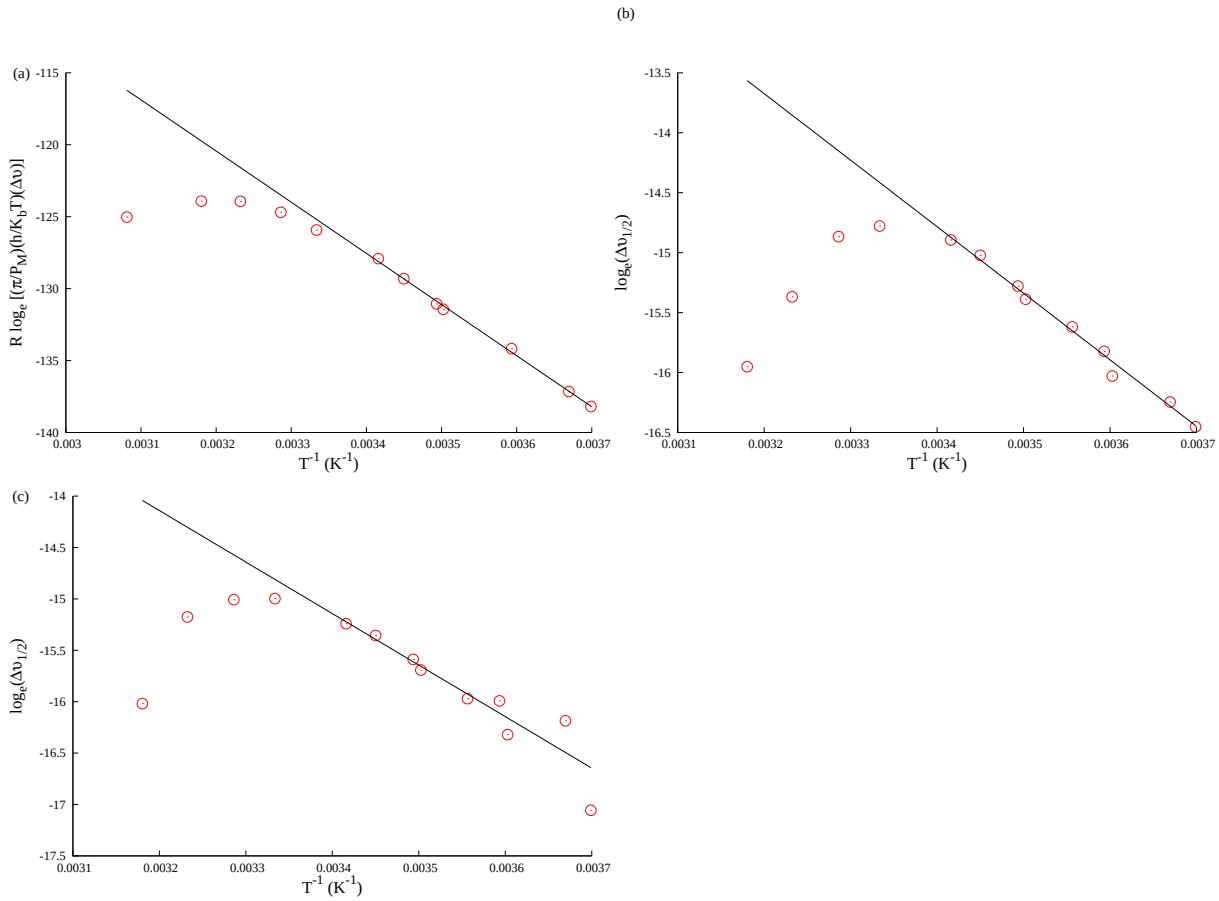

Figure 6: Variable temperature plots for Co^{2+} solutions showing the contribution of specific species to the line width in different samples. (a) $[Co(H_2O)_6]^{2+}$ (10 mM) without any added ligand. (b) Co(II):bpy 1:0.5 ([Co]=10 mM); the contribution of $[Co(H_2O)_6]^{2+}$ to the excess line width has been subtracted over the entire temperature range so that the contribution of $[Co(H_2O)_4(bpy)]^{2+}$ is apparent. (c) Co(II):bpy 1:2.6 ([Co]=10 mM); the contributions of $[Co(H_2O)_6]^{2+}$ and $[Co(H_2O)_4(bpy)]^{2+}$to the excess line width has been subtracted over the entire temperature range so that the contribution of $[Co(H_2O)_2(bpy)_2]^{2+}$ is apparent

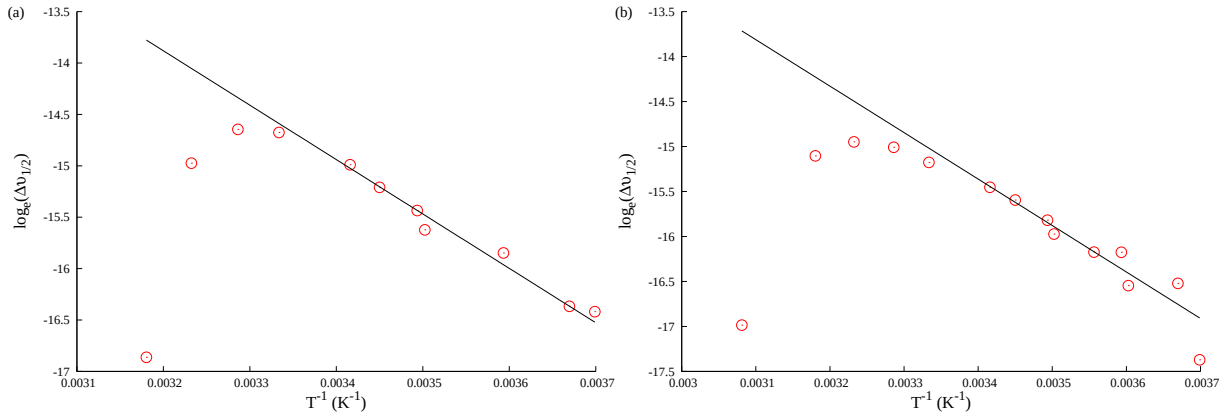

Figure 7: Variable temperature plots for Co^{2+} solutions showing the contribution of specific species to the line width in different samples. (a) Co(II):phen 1:0.5 ([Co]=10 mM); the contribution of $[Co(H_2O)_6]^{2+}$ to the excess line width has been subtracted over the entire temperature range so that the contribution of $[Co(H_2O)_4(phen)]^{2+}$ is apparent. (b) Co(II):phen 1:2.6 ([Co]=10 mM); the contributions of $[Co(H_2O)_6]^{2+}$ and $[Co(H_2O)_4(phen)]^{2+}$to the excess line width has been subtracted over the entire temperature range so that the contribution of $[Co(H_2O)_2(phen)_2]^{2+}$ is apparent

Table 18: Activation parameters for the complexes investigated in this study. The rate constants (k^{298}) were calculated at 298 K using the Eyring-Polanyi equation.

Entry	Species	$\Delta H^{\ddagger}$ ($kJ \cdot mol^{-1}$)	$\Delta S^{\ddagger}$ ($J \cdot mol^{-1} \cdot K^{-1}$)	k^{298} (s^{-1})	Ref.
1	$[Mn(H_2O)_6]^{2+}$	26.8±0.6	-16.2±2.1	$(1.8\pm0.1)\cdot10^7$	This study
2	$[Mn(H_2O)_6]^{2+}$	32.9±1.3	5.7±5.0	$(2.1\pm0.1)\cdot10^7$	Merbach *et al.*[8]
3	$[Mn(H_2O)_6]^{2+}$	36.8±4.2	21±13	$2.3\cdot10^7$	Hunt *et al.*[9]
4	$[Mn(H_2O)_6]^{2+}$	33.9	12.1	$3.1\cdot10^7$	Swift *et al.*[10, 11]
5	$[Mn(phen)(H_2O)_4]^{2+}$	29.6±2.1	-1.5±7.3	$(3.4\pm0.1)\cdot10^7$	This study
6	$[Mn(phen)(H_2O)_4]^{2+}$	38±8	25±29	$2.8\cdot10^7$	Hunt *et al.*[9]
7	$[Mn(phen)_2(H_2O)_2]^{2+}$	31.5±1.4	11.1±5.0	$(7.2\pm0.3)\cdot10^7$	This study
8	$[Mn(phen)_2(H_2O)_2]^{2+}$	38±8	33±38	$7.2\cdot10^7$	Hunt *et al.*[9]
9	$[Mn(bpy)(H_2O)_4]^{2+}$	36.8±2.9	26±10	$(4.9\pm0.3)\cdot10^7$	This study
10	$[Co(H_2O)_6]^{2+}$	35.6±0.7	-6.7±2.6	$(1.6\pm0.1)\cdot10^6$	This study
11	$[Co(H_2O)_6]^{2+}$	46.9±1.2	37.2±3.7	$(3.18\pm0.17)\cdot10^6$	Merbach *et al.*[8]
12	$[Co(H_2O)_6]^{2+}$	33.5	-17.2	$1.35\cdot10^6$	Swift *et al.*[10, 11]
13	$[Co(bpy)(H_2O)_4]^{2+}$	46.1±1.8	33.9±6.1	$(3.1\pm0.1)\cdot10^6$	This study
14	$[Co(bpy)_2(H_2O)_2]^{2+}$	41.7±4.0	16±14	$(2.1\pm0.1)\cdot10^6$	This study
15	$[Co(phen)(H_2O)_4]^{2+}$	44.0±3.7	25±13	$(2.6\pm0.1)\cdot10^6$	This study
16	$[Co(phen)_2(H_2O)_2]^{2+}$	43.0±4.0	18±14	$(1.6\pm0.1)\cdot10^6$	This study

2.4. Computational details

Where crystal structure data was unavailable, structures were optimised using unrestricted density functional theory at PBE0[12]/def2-tzvp[13] with implicit solvation in water using PCM[14] in Gaussian G09 rev D.01. Self-consistent field (SCF) guesses were generated using the fragment guess method to ensure correct spin configuration. The lowest energy spin state was selected by comparing energies at OPBE[15, 16]/def2-tzvp, since OPBE has been found to give qualitatively more reliable results than hybrid exchange-correlation functionals such as PBE0.[17]

Table 19: Energies and bond parameters for computed structures against the level of theory used. Average bond distances were used where there were several different types of water ligands.

Entry	Compound	Spin	Theory	Energy (Hartree)	Bond distance (Å)[a]
1	$[Mn(L1^b)(H_2O)_2]^{2+}$	6	PBE0/def2-tzvp	-2125.49817952	2.260
2	$[Mn(L2^c)(H_2O)_2]^{2+}$	6	PBE0/def2-tzvp	-2085.79597529	2.365
3	$[Co(malonate)(H_2O)_4]^0$	2	PBE0/def2-tzvp	-2104.41408637	2.158
4	$[Co(NH_3)(H_2O)_5]^{2+}$	2	OPBE/def2-tzvp	-1821.56774525	2.140
5	$[Co(NH_3)(H_2O)_5]^{2+}$	4	OPBE/def2-tzvp	-1821.59002942	2.178
6	trans-$[Co(NH_3)_2(H_2O)_4]^{2+}$	2	OPBE/def2-tzvp	-1801.72348057	2.210
7	trans-$[Co(NH_3)_2(H_2O)_4]^{2+}$	4	OPBE/def2-tzvp	-1801.73764909	2.225
8	cis-$[Co(NH_3)_2(H_2O)_4]^{2+}$	2	OPBE/def2-tzvp	-1801.72572591	2.135
9	cis-$[Co(NH_3)_2(H_2O)_4]^{2+}$	4	OPBE/def2-tzvp	-1801.73885187	2.155
10	$[Co(NH_3)(H_2O)_5]^{2+}$	2	PBE0/def2-tzvp	-1820.79646049	2.064
11	$[Co(NH_3)(H_2O)_5]^{2+}$	4	PBE0/def2-tzvp	-1820.82514092	2.108
12	trans-$[Co(NH_3)_2(H_2O)_4]^{2+}$	2	PBE0/def2-tzvp	-1800.94824993	2.103
13	trans-$[Co(NH_3)_2(H_2O)_4]^{2+}$	4	PBE0/def2-tzvp	-1800.97194756	2.130
14	cis-$[Co(NH_3)_2(H_2O)_4]^{2+}$	2	PBE0/def2-tzvp	-1800.94895084	2.138
15	cis-$[Co(NH_3)_2(H_2O)_4]^{2+}$	4	PBE0/def2-tzvp	-1800.97289861	2.123

[a] Metal-to-oxygen distance. [b] L1 refers to 3,12,18-triaaza-6,9-dioxabicyclo[12.3.1]octadeca-1(18),14,16-triene. [c] L2 is 6,9-dioxa-3,12,18-triazabicyclo[12.3.1]octadeca-1(18),14,16-triene.

2.5. Crystallographically determined bond lengths

Table 20: Bond parameters obtained from crystal structures. Average bond distances were used where there were several different types of water ligands.

Entry	Compound	M-O bond distance (Å)[a]	Reference
1	$[Mn(H_2O)_6]^{2+}$	2.196	[18]
2	$[Mn(bpy)(H_2O)_4]^{2+}$	2.166	[19]
3	$[Mn(phen)(H_2O)_4]^{2+}$	2.173	[20]
4	$[Mn(phen)_2(H_2O)_2]^{2+}$	2.139	[21]
5	$[Mn_4(P_2W_{15}O_{56})_2(H_2O)_2]^{16-}$	2.240	[22]
6	$[Mn(L_3)(H_2O)_2]^{2+}$	2.261	[23]
7	$[Mn(EDTA)(H_2O)]^{2-}$	2.241	[24]
8	$[Mn(TMDTA)(H_2O)_2]^{2-}$	2.154	[25]
9	$[Co(H_2O)_6]^{2+}$	2.082	[26]
10	$[Co(bpy)(H_2O)_4]^{2+}$	2.082	[27]
11	$[Co(bpy)_2(H_2O)_2]^{2+}$	2.070	[28]
12	$[Co(phen)(H_2O)_4]^{2+}$	2.097	[29]
13	$[Co(phen)_2(H_2O)_2]^{2+}$	2.077	[30]
14	$[Co_4(P_2W_{15}O_{56})_2(H_2O)_2]^{16-}$	2.090	[6]
15	$[Co_4(PW_9O_{34})_2(H_2O)_2]^{10-}$	2.150	[6]

[a] Metal-to-oxygen distance. [b] L3 is 2,13-dimethyl-3,6,9,12,18-pentaazabicyclo[12.3.1]-octadeca-1(18),14,16-triene.

References

[1] R. F. Bogucki, G. McLendon, A. E. Martell, *J. Am. Chem. Soc.* **1976**, *98*, 3202–3205.

[2] L. Alderighi, P. Gans, A. Ienco, D. Peters, A. Sabatini, A. Vacca, *Coord. Chem. Rev.* **1999**, *184*, 311–318.

[3] G. von Anderegg, *Helv. Chim. Acta.* **1963**, *46*, 2813–2822.

[4] R. L. Davies, K. W. Dunning, *J. Chem. Soc.* **1965**, 4168–4185.

[5] T. Williams, C. Kelley, http://sourceforge.net/projects/gnuplot/, **2014**.

[6] C. A. Ohlin, S. J. Harley, J. G. McAlpin, R. K. Hockin, B. Q. Mercado, R. L. Johnson, E. M. Villa, M. K. Fidler, M. M. Olmstead, L. Spiccia, R. D. Britt, W. H. Casey, *Chem. Eur. J.* **2011**, *17*, 4408–4417.

[7] R. Sharma, J. Zhang, C. A. Ohlin, *Dalton Trans.* **2015**, *44*, 19068–19071.

[8] Y. Ducommun, K. E. Newman, A. E. Merbach, *Inorg. Chem.* **1980**, *19*, 3696–3703.

[9] M. Grant, H. W. Dodgen, J. P. Hunt, *Inorg. Chem.* **1971**, *10*, 71–73.

[10] T. J. Swift, R. E. Connick, *J. Chem. Phys.* **1962**, *37*, 307–320.

[11] T. J. Swift, R. E. Connick, *J. Chem. Phys.* **1964**, *41*, 2553–2554.

[12] C. Adamo, V. Barone, *J. Chem. Phys.* **1999**, *110*, 6158–6159.

[13] F. Weigend, R. Ahlrichs, *Phys. Chem. chem. Phys.* **2005**, *7*, 3297–3305.

[14] J. Tomasi, B. Mennucci, R. Cammi, *Chem. Rev.* **2005**, *105*, 2999–3093.

[15] N. C. Handy, A. J. Cohen, *Mol. Phys.* **2001**, *99*, 403–412.

[16] W.-M. Hoe, A. Cohen, N. C. Handy, *Chem. Phys. Lett.* **2001**, *341*, 319–328.

[17] M. Swart, *Chem. Phys. Lett.* **2013**, *580*, 166–171.

[18] D. Sivanesan, S. Kanan, T. D. Thangadurai, K.-D. Jung, S. Yoon, *Dalton Trans.* **2014**, *43*, 11465–11469.

[19] W. M. Singh, J. B. Baruah, *Inorg. Chim. Acta* **2009**, *362*, 4268–4271.

[20] l.-F. Ma, L.-Y. Wang, S.-H. Chen, H.-W. Hou, S. R. Batten, *Polyhed.* **2009**, *28*, 2494–2502.

[21] M. Du, C.-P. Li, X.-J. Zhao, Y. Q., *Cryst. Eng. Comm.* **2007**, *9*, 1011–1028.

[22] C. J. Gómez-Gárcia, J. J. Borrś-Almenar, E. Coronado, L. Ouahab, *Inorg. Chem.* **1994**, *33*, 4016–4022.

[23] G. F. Liu, M. Filipovic, F. W. Heinemann, Ivanović-Burmazović, *Inorg. Chem.* **2007**, *46*, 8825–8835.

[24] X. F. Wang, J. Gao, Z. H. Zhang, Y. F. Wang, L. J. Chen, W. Sun, X. D. Zhang, *Z. Struk. Khimii* **2008**, 753.

[25] U. Rychlewska, B. Warżajtis, D. Cvetić, D. D. Radanović, D. Gurešić, M. I. Djuran, *Polyhed.* **2007**, *26*, 1717–1724.

[26] S. M. Mobin, A. Mohammad, *Dalton Trans.* **2014**, *43*, 13032–13040.

[27] N. Lian, Z. adnd Zhao, J. Zhang, Y. Gu, X. Li, B. Tang, *Z. Krist.-New Cryst. St.* **2009**, *224*, 329.

[28] V. Ciornea, L. Minalieva, J. P. Costes, G. Novitchi, I. Filipova, R. T. Galeev, S. Shova, V. K. Voronkova, A. Gulea, *Inorg. Chim. Acta* **2008**, *361*, 1947.

[29] Z. G. Li, G. H. Wang, J. W. Niu, N. H. Hu, *Acta Crystallogr. Sect. C* **2007**, *63*, m94–m96.

[30] R. Carballo, B. Covelo, E. M. Vázquez-López, E. Garćia-Martínez, *Z. Anarg. Allag. Chem.* **2003**, *629*, 244–248.